

Low Earth Orbit Constellation Design Using the Earth-Moon L1 Point

Naomi Chow, Erica Gralla, N. J. Kasdin, *Princeton University**
James Chase, *Jet Propulsion Laboratory*†

Over the last decade, there has been a growing interest in the development of low earth orbit (LEO) microsatellite constellations for commercial, strategic, and scientific purposes. High costs present a major obstacle to the development of such constellations; launch costs, in particular, may represent as much as 40% of the life-cycle cost. Deployment of satellites into different orbital planes generally requires separate launch vehicles, so several smaller launches are required for a single constellation. We propose to reduce costs by using a single large launch vehicle to carry an entire fleet of microsatellites to the Earth-Moon L1 Lagrange point. By taking advantage of the complex dynamical behavior at this location, the microsatellites can be returned to multiple Earth orbital planes via aerocapture, using minimal ΔV . This paper presents a proof of concept and feasibility assessment of such a system, demonstrating 38% cost savings for a baseline mission.

INTRODUCTION

Both the space industry and government have displayed a growing interest in using satellite constellations for continuous global coverage. Unfortunately, the high cost of such missions presents a significant problem to these developers. To reduce these costs, designers have been turning to small lightweight microsatellites. While this reduces the satellite cost, launch costs remain unaddressed. For satellite constellations in multiple orbit planes, launch costs can become prohibitively expensive. Single launches are limited by the need to perform plane changes and vary the longitude of the ascending node. A 60 degree single-impulse plane change, for example, requires as much ΔV as the launch into low earth orbit (LEO).² This leads to the need for multiple launches (one per plane). While the use of lightweight microsatellites reduces the launch mass considerably, the requirement for multiple launches keeps costs high. In fact, the cost of multiple launches may represent up to 40% of the life-cycle cost.¹ Thus, there is a clear need for new launch methods that would reduce the number of launch vehicles required. This study investigates one such method, using a single large launch vehicle and distributing the spacecraft throughout various Earth orbital planes by utilizing the dynamics of the Earth-Moon L1 Lagrange point and employing an aerocapture maneuver to inject into the final orbit. The method offers significant cost savings for several types of satellite constellations.

* Naomi Chow and Erica Gralla, senior engineering students, N.J. Kasdin, Assistant Professor, Princeton University, Princeton, NJ 08544.

† James Chase, Staff Engineer for Mission and Systems Architecture, NASA Jet Propulsion Laboratory, 4800 Oak Grove Drive, Pasadena, CA91109.

Proposed Constellation Design Using the Earth-Moon L1 Point

One possible method of reducing the cost of current constellation designs is to minimize the number of launch vehicles needed. However, as mentioned earlier, the high ΔV cost of using propulsive maneuvers to change a spacecraft's inclination and ascending node after deployment makes this method unattractive and in some cases unaffordable. The following design suggests an alternative method for distributing spacecraft to various orbital planes.

The design takes advantage of the complex dynamical behavior near the Earth-Moon L1 Lagrange point. From a Lissajous orbit about L1, it is possible, using minimal ΔV , to access various Earth orbital planes with different inclinations and ascending nodes.. Thus, a single launch vehicle can carry an entire fleet of spacecraft to L1; from this location, they can be returned to multiple Earth orbital planes.

Aerocapture is then employed to bring the spacecraft into LEO. Aerocapture involves the use of atmospheric drag to slow the spacecraft and insert it into orbit, followed by small propulsive burns to raise perigee and circularize the orbit. This maneuver reduces the amount of fuel required, compared to a purely propulsive orbit insertion.

SYSTEMS ANALYSIS

Summary

Figure 1 provides an overview of the proposed architecture. Several carrier spacecraft (each carrying a set of microsattellites to be deployed in a single orbital plane) are launched on a single launch vehicle to the Earth-Moon L1 point and inserted into a Lissajous orbit. From this point, carriers return on separate Earth-bound trajectories leading to different orbital planes. Each carrier performs an aerocapture maneuver and a circularizing burn to reach LEO. Following the orbit insertion, the satellites are phased to distribute them within the orbital plane. The following is a summary of the preliminary systems analysis into the feasibility of such a mission architecture. In the remainder of this section we present a more detailed description of the supporting analysis.

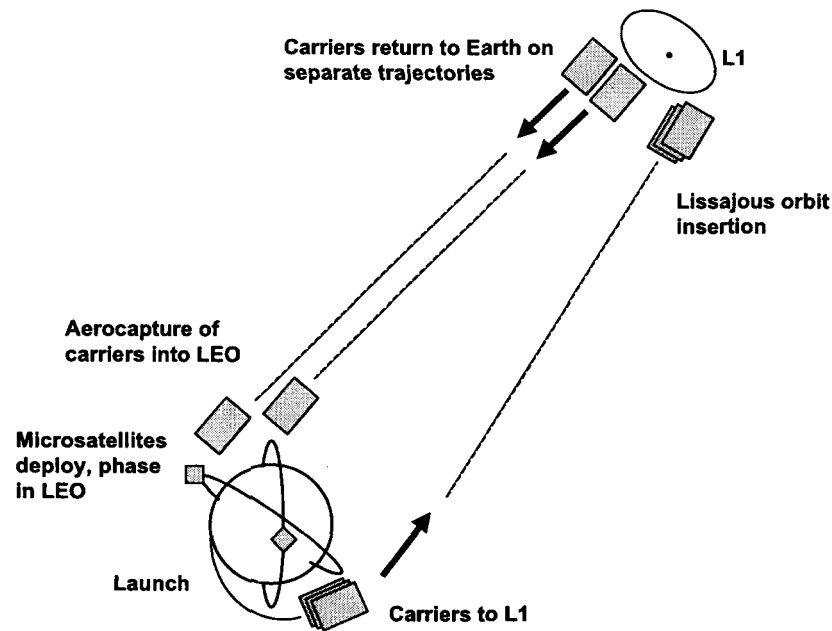


Figure 1: Overview

In this analysis, we do not consider the design of the microsattellites; we assume a 75 kg mass, including payload, all subsystems, and propellant for phasing, orbit maintenance, and attitude control. The carrier spacecraft consist of supporting structures for the microsattellites, a liquid bipropellant propulsion system, and a ballute for aerocapture, along with the standard required subsystems. The carrier spacecraft propellant budget includes fuel for Lissajous orbit insertion and departure and LEO circularization after aerocapture. The launch vehicle sends all the carriers on the L1-bound trajectory. The transfer time to L1 is about 4 days. After Lissajous orbit insertion, carrier vehicles may remain at L1 as long as necessary in order to return on a trajectory with the correct final inclination and ascending node. From L1, carrier vehicles can access Earth orbits with any ascending node and inclinations up to approximately 60 degrees. To slow each carrier vehicle from the return transfer orbit into LEO, aerocapture is used in order to reduce ΔV costs. A ballute is deployed to minimize atmospheric heating and drag during aerocapture, and a final ΔV maneuver raises perigee to reach a circular orbit. The individual microsattellites are deployed from the carrier spacecraft and distributed within the final orbital plane over the course of approximately 36 days.

The following sections examine relevant trajectory design issues. The trajectory includes a transfer from Earth to a Lissajous orbit about L1, a return transfer from the L1 orbit to Earth, aerocapture into the final Earth orbit, and phasing of satellites within each orbital plane (see Figure 2). Our analysis of the trajectory is quite limited; we have used a simple patched conics approach to investigate the 'worst case' ΔV costs. Thus, we provide only a brief overview of the challenges associated with each of these components.

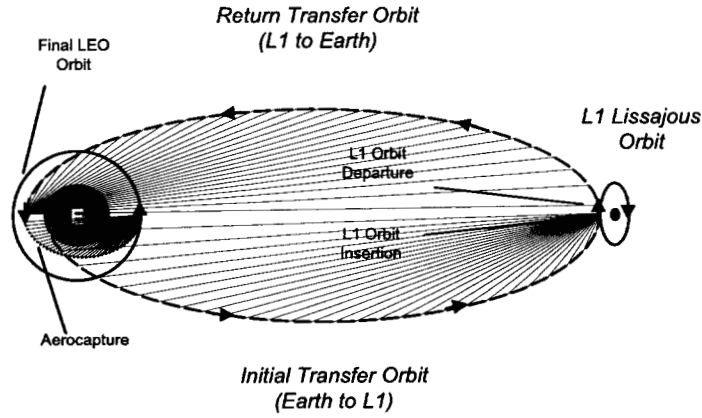


Figure 2: Trajectory Overview

L1 Dynamics

In order to model the Lissajous orbit about the Earth-Moon L1 point, we utilize the linear approximation of the equations of motion near the L1 point based on the restricted three-body problem (see Refs. 4, 5, and 6). A rotating coordinate system is chosen with the origin at L1, the ξ -axis pointing toward the Moon and the ζ -axis out of plane (see Figure 2); units are non-dimensionalized such that the angular velocity of L1 about Earth, the sum of the masses of the primaries, and the distance from L1 to the Moon are equal to unity. The distance from L1 to the Moon is represented by γ , and μ denotes the ratio of the gravitational constant of the Moon to the sum of the gravitational constants of both primaries.

$$\begin{aligned}
 \ddot{\xi} - 2\dot{\eta} - (1 + 2c)\xi &= 0 \\
 \ddot{\eta} + 2\dot{\xi} + (c - 1)\eta &= 0 \\
 \ddot{\zeta} + c\zeta &= 0
 \end{aligned} \tag{1}$$

$$c = \frac{\mu}{\gamma} + \frac{1 - \mu}{(1 - \gamma)^3} \tag{2}$$

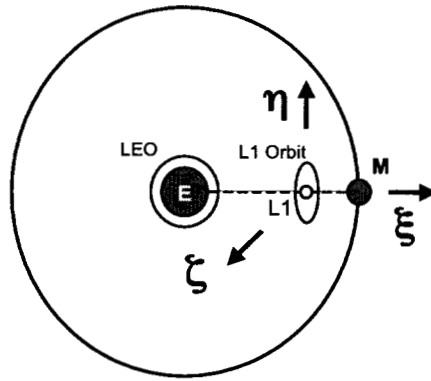


Figure 3: L1-Centric Coordinate System

The linearized equations of motion (1) admit periodic, stable, and unstable solutions. Lissajous orbits are achieved by choosing initial conditions in order to obtain periodic motion. With this restriction, the solution can be written as follows, where the a's and b's represent constants and ω and ω_z represent the frequencies of motion.⁴

$$\begin{aligned}
 \xi &= a_1 \cos \omega t + a_2 \sin \omega t \\
 \eta &= -b a_1 \sin \omega t + b a_2 \cos \omega t \\
 \zeta &= a_3 \sin \omega_z t + a_4 \cos \omega_z t
 \end{aligned}
 \tag{3}$$

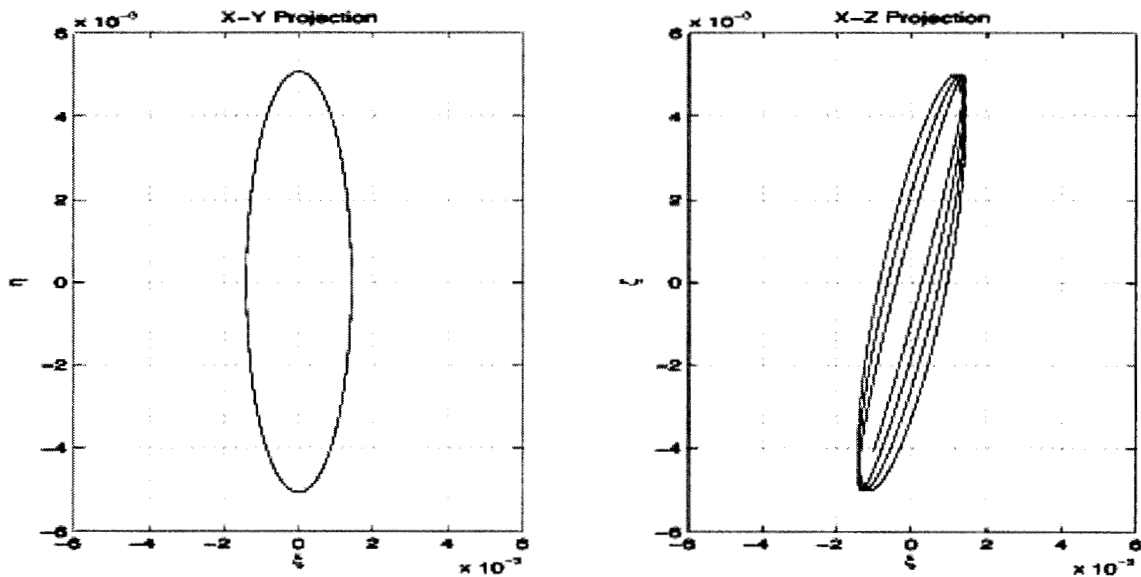


Figure 4: Lissajous Orbit About L1

The out-of-plane motion (ζ) is independent of the in-plane motion, so a small ΔV at orbit insertion can instigate out-of-plane motion, enabling inclination changes.

Therefore, from a Lissajous orbit about L1 (see Figure 4), a wide range of Earth orbital planes can be reached. In this analysis, we assume that a ΔV of 630 m/s tangent to the motion shifts the spacecraft from the L1 orbit to an elliptical transfer orbit back to Earth (discussed below). The ascending node of the final Earth orbit can be varied by changing the timing of the return transfer. Furthermore, because of the out-of-plane motion instigated at L1 orbit insertion, the return transfer orbit is in a different orbital plane. We can plot the Earth orbit inclination achievable using a burn at any point in the L1 orbit by transforming the coordinate system from L1-centric to Earth-centered inertial (ECI) coordinates (in which the x - y plane is the Earth equatorial plane) and adding the ΔV to access the return transfer orbit. The transformation to ECI coordinates is given as follows:

$$\begin{aligned}\bar{r} &= \bar{R} + \bar{\rho} \\ \bar{v} &= \dot{\bar{\rho}} + \bar{\Omega} \times \bar{R} + \bar{\Omega} \times \bar{\rho} + \Delta V\end{aligned}\tag{4}$$

In the above equations, R represents the position vector of L1 in ECI coordinates, ρ is the position vector of the spacecraft in the L1-centered frame, and Ω is the angular velocity of L1 about the Earth. To find R and Ω , we assume the Moon's orbit is circular and use an average inclination of 23 degrees. We find ρ and $d\rho/dt$ from Eqs. (1) in the L1 frame. Adding the tangent 630 m/s ΔV , the inclination in the equatorial ECI frame is found using the position and velocity from Eq. (4) according to:

$$\begin{aligned}\bar{h} &= \bar{r} \times \bar{v} \\ i &= \cos^{-1}\left(\frac{\bar{h} \cdot \hat{k}}{|\bar{h}|}\right)\end{aligned}\tag{5}$$

The above equations give the inclination with respect to the Earth's equatorial plane of a spacecraft exiting the L1 orbit. Figure 5 shows the inclination as a function of time to demonstrate the variation in achievable Earth orbit inclinations, depending on the timing of the exit from L1 orbit.

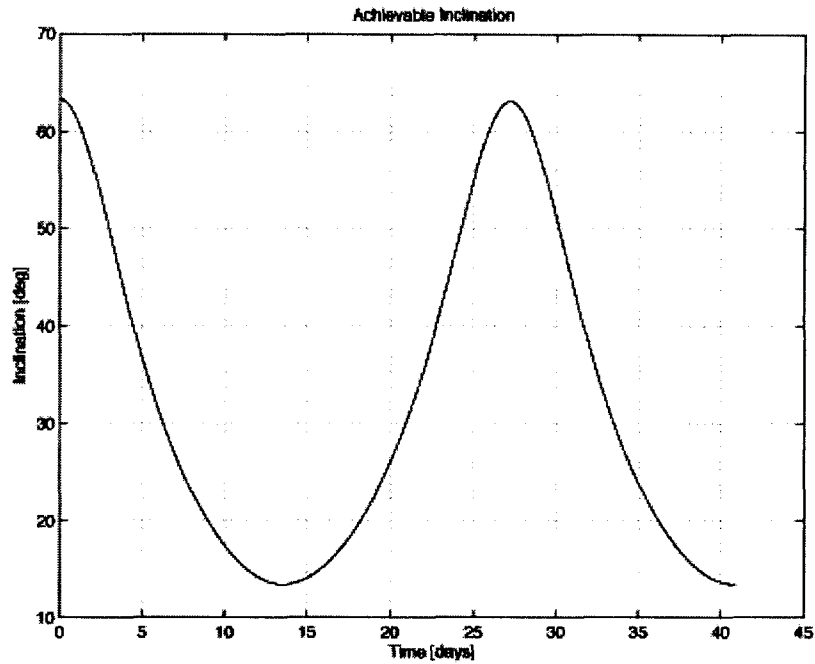


Figure 5: Inclination As a Function of Time

The linear approximation used here to model Lissajous orbits is valid only at short distances from L1, so we have used a patched conics approach and elliptical orbits to analyze the ΔV costs associated with transfer to and from L1. A more precise approach utilizes the nonlinear dynamics and makes use of the stable and unstable manifolds leading to and from L1, in order to reduce the transfer ΔV requirements (for example, see Ref. 4). We leave this to a later analysis.

Aerocapture

Aerocapture slows the spacecraft from the elliptical transfer orbit into the final Earth orbit. Aerocapture, an aeroassist maneuver, is the use of aerodynamic drag to bring a vehicle from an interplanetary flyby trajectory into a parking orbit in a single pass (see Figure 6). Instead of firing thrusters to slow the vehicle and bring it into orbit, aerocapture inserts the vehicle into the atmosphere, which produces enough drag in one pass to provide deceleration of several kilometers per second. By taking advantage of atmospheric drag, aerocapture reduces the velocity of the spacecraft without using a significant amount of propellant.

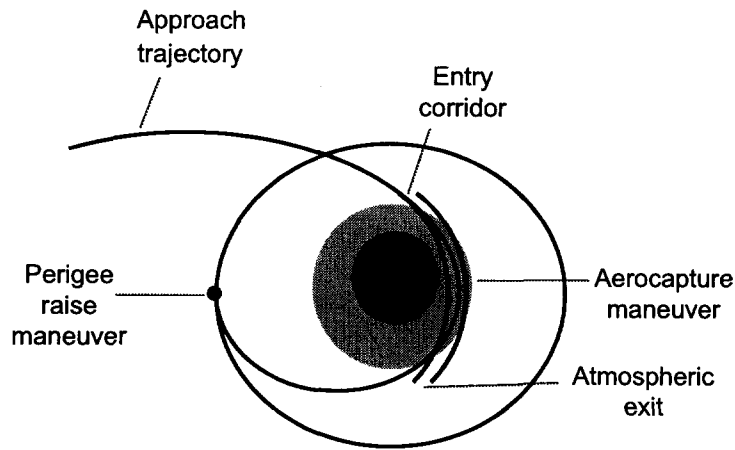


Figure 6: Aerocapture

There exists a fairly narrow entry corridor for successful aerocapture. If directed into too steep of an atmospheric entry, the vehicle may not be able to exit the atmosphere and reach the desired parking orbit. Consequently, the vehicle will experience high thermal loads and aerodynamic forces and will either overheat or crash into the surface. Conversely, at too shallow of an atmospheric pass, the vehicle may not dissipate enough energy and will not capture into the parking orbit; instead, it will continue in a heliocentric orbit. The upper bound of the entry corridor (highest altitude) represents the shallowest trajectory that leads to successful capture, while the lower bound marks the steepest trajectory that still manages to exit the atmosphere and reach the parking orbit. To carefully control this entry phase as well as the subsequent exit from the atmosphere, the spacecraft must have adequate guidance, control, and maneuvering capabilities. Clearly, a single-pass capture of the microsattellites into LEO seems efficient, but the significant thermal loading and need for accuracy of control suggest the consideration of another aeroassist maneuver.

Aerobraking also takes advantage of atmospheric drag to slow the spacecraft, but it requires multiple passes (see Figure 7). The orbit apogee decreases with each subsequent pass, circularizing and lowering the spacecraft's orbit over time. A smaller ΔV is required for the eventual circularization (perigee raise), but aerobraking can require hundreds of passes.

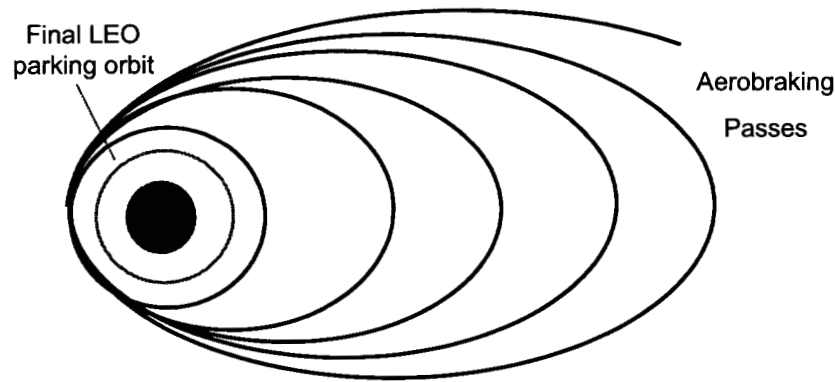


Figure 7: Aerobraking

Comparing these two aeroassist maneuvers, we see that purely ballistic aerocapture can have large margins of error. Aerobraking, however, does not require such a precise entry corridor, because of the many passes involved. With deceleration spread out over multiple passes, lower aerodynamic and thermal loads are experienced.

A major concern associated with aerobraking, however, is that of radiation exposure during passes through the high-radiation Van Allen belts. Since hundreds of passes may be required, sensitive components on the microsattellites could be damaged. Even with the microsattellites housed in a carrier vehicle, designing to withstand significant radiation exposure requires heavier and more expensive materials. We therefore prioritize avoidance of the Van Allen belt over reduction of aerodynamic and thermal loads and select a single-pass aerocapture.

Despite the significant amount of atmospheric drag, the carrier spacecraft requires additional hardware to slow it down as it approaches Earth. A ballute, or cross between a balloon and a parachute, increases the surface area of the spacecraft in contact with the atmosphere, increasing drag on the vehicle. The inflatable ballute is constructed of durable, thin, and lightweight materials. We estimate a ballute system mass of 50-100 kg for each carrier vehicle.⁹

Trajectory Design

Launch. Initially, we assume launch on a Delta IV-Heavy launch vehicle. The $C3$ (hyperbolic launch energy) required for launch is used to determine the launch vehicle capability. Eq. (6) defines $C3$ in a two-body system, where ϵ is the specific mechanical energy, μ_E is the Earth gravitational parameter, and a denotes the semi-major axis of the elliptical transfer orbit to L1. Using Eq. (6) for the desired L1 destination and neglecting three-body effects, the $C3$ for a Earth-Moon L1 trajectory is $-2.4 \text{ km}^2/\text{s}^2$ (For the two-body Keplerian analysis, a negative $C3$ represents bound orbits and a $C3$ of zero represents a parabolic escape.). An analysis of three-body dynamics (including the

effects of the Moon) verifies that this $C3$ is sufficient for transporting the carrier vehicles to the L1 point.

$$C3 = 2\varepsilon = -\mu_E / a \quad (6)$$

A small amount of ΔV must be budgeted to correct the launch injection error. For the Delta IV, three sigma accuracies may be extrapolated to be ± 5.6 km for the perigee altitude, ± 810 km for the apogee altitude, and ± 0.03 degrees for the inclination.⁵ Using these numbers, a ΔV on the order of 10 m/s is calculated.

Transfer to Lissajous Orbit. An in-plane elliptical transfer orbit with an apogee at the L1 point is used to model the transfer to L1. At orbit insertion, a ΔV of 1.5 m/s in the ζ -direction is required to instigate out-of-plane motion. The velocity of the spacecraft in the L1 orbit is on the order of 2.4 m/s. The velocity of the spacecraft at apogee of the transfer orbit is calculated using Eq. (7) below, where a represents the semi-major axis and r the position of the spacecraft. Taking into account the orbital velocity of the L1 point about the Earth, the ΔV required for orbit insertion is approximately 634 m/s.

$$v^2 = \mu \left(\frac{2}{r} - \frac{1}{a} \right) \quad (7)$$

Return Transfer to Earth. By the same Eq. (7), the ΔV required to leave L1 orbit and access the return transfer elliptical orbit to Earth is 631 m/s (the perigee of the return orbit is slightly lower because of aerocapture, but the difference in ΔV is negligible). As discussed above, this ΔV is assumed tangent to the spacecraft's motion; thus, the spacecraft leaves in a transfer orbit at a different inclination, leading to a different Earth orbital plane.

Aerocapture. Aerocapture slows the spacecraft from the elliptical transfer orbit into the final Earth orbit. With an aerocapture orbit perigee of 100 km, we can achieve a 2890 m/s ΔV savings (from Eq. 7). A circularization burn of 233 m/s is required to raise perigee after the aerocapture maneuver (also from Eq. 7). The total ΔV requirement for the aerocapture phase is thus only 233 m/s.

Phasing. The phasing of satellites within each orbital plane is accomplished by sending the carrier vehicle to a lower altitude than the final desired microsatellite altitude. At this lower altitude, the carrier vehicle has a shorter orbital period and therefore can phase the deployment of the microsattellites over the course of several days. Minimizing the altitude difference of the carrier and microsatellite orbits reduces the amount of ΔV necessary but increases the time required for phasing. In this proof-of-concept mission, we seek to minimize ΔV , so we will assume that a phasing period of approximately one month is acceptable.

We can find the phasing ΔV requirements for a final orbit altitude of 1000 km (carrier altitude of 980 km). Using Eq. (7), the total ΔV for deploying each satellite from its carrier vehicle is 10 km/s. The carrier at a lower altitude will travel 10 degrees more per day than the satellites at the higher altitude, allowing complete phasing of the satellites in approximately 36 days (see Figure 8).

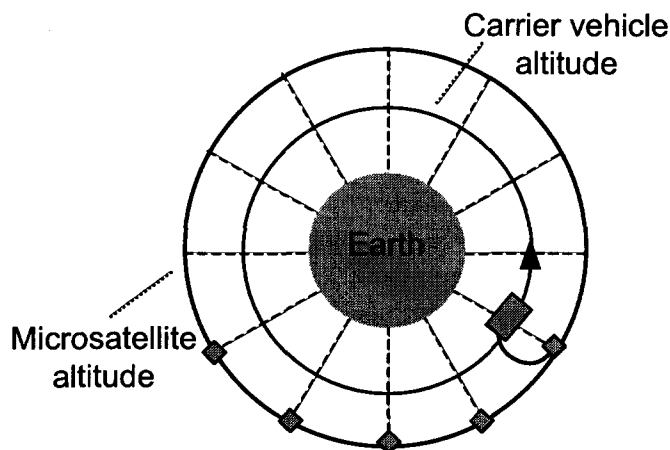


Figure 8: Satellite Phasing Within Orbital Plane

The total ΔV cost for the mission is summarized in Table 1. Because it is calculated using patched conics, this total is the ‘worst case’ ΔV cost. By taking advantage of the stable and unstable manifolds leading to and from the L1 point, we expect that ΔV requirements can be significantly reduced.

**Table 1
 ΔV SUMMARY**

Event	ΔV [m/s]
Launch injection error	10
L1 orbit insertion	634
Gravity losses (1%)	6
L1 orbit maintenance	5
L1 orbit departure	631
Gravity losses (1%)	6
Aerocapture circularization	233
Total:	1525

COST ANALYSIS

The previous section describes the proposed method for constructing global microsatellite constellations using the Earth-Moon L1 point. The question remains whether this new approach is better than the traditional ‘direct launch’ approach using

multiple launch vehicles. In order to compare the two methods, we examine the two approaches from systems cost perspective. The following four sections describe our assumptions and present an approximate cost comparison.

Assumptions

Constellations types range from a few satellites in high altitude polar orbits to large clusters of satellites at lower altitudes and inclinations. Rather than examine a single type of constellation (that might misrepresent many alternative configurations), it is more useful to look at a large envelope of possible configurations. In describing a constellation, four key parameters are considered, which are shown in Table 2. The table shows each parameter, along with its respective minimum, maximum, and baseline margins used in this study.

Table 2
CONSTELLATION DESIGN PARAMETERS

	Minimum	Maximum	Baseline
Number of Planes	1	10	6
Number of s/c per plane	1	20	8
Altitude	200 km	2000 km	1000 km
Inclination	30 deg	90 deg	60 deg

In this analysis, satellite constellations beyond LEO are not considered, and all satellites are assumed to be microsattellites with masses ranging from 10 to 135 kg. All orbital planes are assumed to be at the same inclination in each constellation (only the longitude of the ascending node is varied).

Traditional Direct Launch Method

The traditional launch method for satellite constellations requires one launch vehicle per orbital plane, chosen based on the payload mass and orbit requirements. The payload mass consists of the microsattellites and the required hardware for their interface and deployment. The interface hardware mass is conservatively estimated to be 25% of the payload mass. A summary of these system elements is presented in Table 3. After deployment, the microsattellites use thrusters to distribute themselves within the orbital plane. In this manner, the constellation is launch in a relatively simple fashion, but at a high cost due to the number of required launch vehicles.

Table 3
DIRECT ENTRY SYSTEM ELEMENTS

System Element	Number Required	Mass Estimate
Launch Vehicle (LV) Capability	1 per orbital plane	KSC website ³
Interface & Deployment Hardware	1 per LV	25% of launch mass
Microsattellites	1 to 20 per LV	75 kg

Proposed L1 Trajectory Launch Method

The proposed trajectory requires a carrier vehicle instead of hardware for interface and deployment. The carrier vehicle must navigate to and from the Earth-Moon L1 point and perform an Earth aerocapture maneuver; thus, although less sophisticated than a fully functional spacecraft, most of the standard subsystems are required. The ΔV budget suggests that a bipropellant propulsion system is needed, along with additional structure to support large propellant tanks.

Table 4 describes these system elements, along with the number of units required and method of mass estimation. A detailed ΔV budget is used in conjunction with the payload mass to size the carrier vehicle, using standard size estimates for each subsystem.¹⁰ While a single launch vehicle for the entire constellation would be most desirable, for this analysis we allow up to three launch vehicles for a given constellation. Despite the increased complexity of spacecraft system design, our proposed launch approach offers the potential to significantly reduce costs due to the use of fewer and larger (more cost-efficient) launch vehicles.

Table 4
CARRIER VEHICLE SYSTEM ELEMENTS

System Element	Number Required	Mass Estimate
Launch Vehicle	1 to 3	From KSC website ³
Carrier Vehicle	1 per orbital plane	-
Payload mass	-	Sum of microsattellites
ACS, telecom, power, thermal, structures, etc.	-	80% of payload mass ¹⁰
Biprop. propulsion system	-	18% of propellant mass ¹⁰
Propellant mass	-	Determined from ΔV budget and Isp of 315 ¹⁰
Ballute mass	-	50 to 100 kg ⁹
Microsattellites	1 to 20 per carrier vehicle	75 kg

Cost Analysis and Comparison

A spreadsheet model is used to compare costs for the two approaches outlined above, producing an overall percentage cost savings for each constellation type considered. The model, outlined in Figure 9 and described in Table 5, is composed of eleven modules. We utilize standard mass/power estimates and orbital mechanics equations,¹⁰ supplemented by the RSDO spacecraft catalog¹¹ and a launch vehicle database (described below). This analysis uses scaling factors and iterative calculations for system optimization.

For each of the two approaches, costs are calculated by adding the total cost of the launch vehicles and carrier vehicles (or deployment hardware). Launch vehicle costs are

estimated using approximate figures from the NASA procurement office and carrier vehicle costs are obtained by analogy to the RSDO spacecraft catalog.¹¹ In general, launch vehicle costs range from approximately \$25M to \$150M. The cost of deployment hardware falls between \$1M and \$18M, depending on the size and number of microsattellites. The carrier vehicle cost can range from \$15M to \$70M, which includes an allocation of \$10M for the bipropellant propulsion system. For this comparison, all other costs either cancel out (i.e. same microsattellite cost in both approaches) or are negligible (i.e. integration costs). From these estimates, the percentage of overall cost savings can be calculated.

Table 5
COST MODULES

Cost Module	Description	Type	Source
Constellation Design	Planes, satellites, altitude & inclination	User input	-
ΔV Budget	Launch C3 and maneuvers for L1 orbit insertion, aerobraking, phasing, and orbit control	User input (fixed)	Calculated in <i>Trajectory Design</i>
Microsatellite Design	Mass equipment list including propulsion, structures, and payload allocations	User input (variable)	Propellant mass based on s/c mass & ΔV
Carrier Vehicle Design	Cost and mass equipment list including payload, ballute, propulsion, ACS, etc.	Analysis (scaling)	Wertz & Larson ¹⁰ and RSDO Spacecraft Catalog ¹¹
Propellant Mass Sizing	Iterative analysis for determining final propellant mass	Analysis	Wertz & Larson ¹⁰
Interface & Deployment Hardware	Cost and mass equipment list including structures and deployment mechanism	Analysis (scaling)	Wertz & Larson ¹⁰
Launch Vehicle Performance	Cost and mass for all approved NASA launch vehicles based on desired orbit	Database	KSC website ³ and internal JPL resources
Direct Trajectory Sys. Analysis	Complete system description including all ΔV s, masses, and costs	Analysis	Wertz & Larson ¹⁰
L1 Trajectory Systems Analysis	Complete system description including all ΔV s, masses, and costs	Analysis	Wertz & Larson ¹⁰
Lowest Cost LV Analysis	Determines what combination of 1-3 launch vehicles has the lowest cost	Analysis	-
Cost Savings (%)	Displays the cost savings for all combinations of # of planes vs. spacecraft	Analysis	-

First, we examine the variation in cost savings over the types of constellations outlined above (varying the number of planes and satellites), at a constant inclination and altitude (60 deg, 1000 km). The cost savings are charted in Table 7. Dark gray indicates a cost savings of 30% or more, light gray shows savings less than 30%, and white indicates negative savings. The results vary greatly, with quite significant cost savings in some areas (such as the baseline mission chosen above), and negative savings in others. The variability is driven by the launch vehicle cost; slight changes in payload mass can necessitate a larger launch vehicle, and thus a higher cost. As expected, types A and B show much less savings. On average, the savings are 3%, 6%, 20%, and 21% for types A, B, C, and D, respectively. Thus, for certain types of microsatellite constellations, significant savings can be realized.

Table 7
SAVINGS FOR VARIOUS CONSTELLATION TYPES
(1000 km altitude, 60 deg inclination)

# of Planes	# of Microsatellites per Plane							
	1	2	4	6	8	10	12	14
3	TYPE A 3% Avg. Savings				TYPE B 6% Avg. Savings			
4								
5								
6								
7	TYPE C 20% Avg. Savings				TYPE D 21% Avg. Savings			
8								
9								
10								

We also examine the variation in percentage savings for constellations at various altitudes. The results are plotted in Figure 10. Savings are much more significant at higher orbit altitudes because larger launch vehicles required for launching each orbital plane (in the direct launch method) for higher altitude constellations.

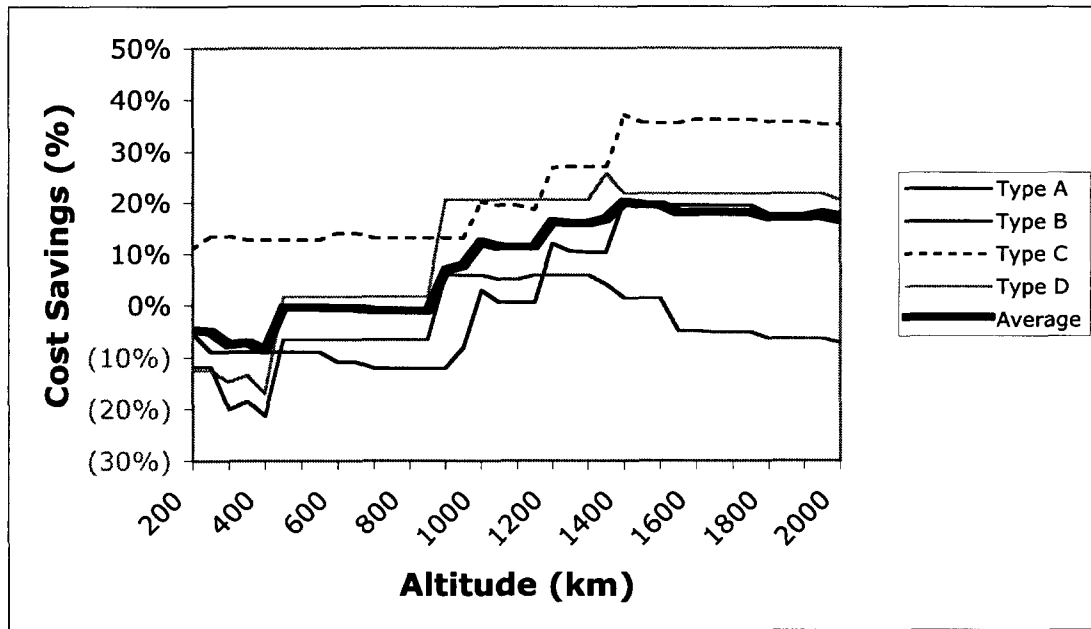


Figure 10: Cost Savings With Respect to Orbit Altitude

Similarly, the variation in percentage savings for constellations at various inclinations is plotted in Figure 11. The step function is due to the change in launch vehicle for the direct launch method; at around 55 degrees, the required launch vehicle changes from a Taurus to a Delta II, generating increased cost. Thus, savings are much higher at larger orbit inclinations for all types of constellations.

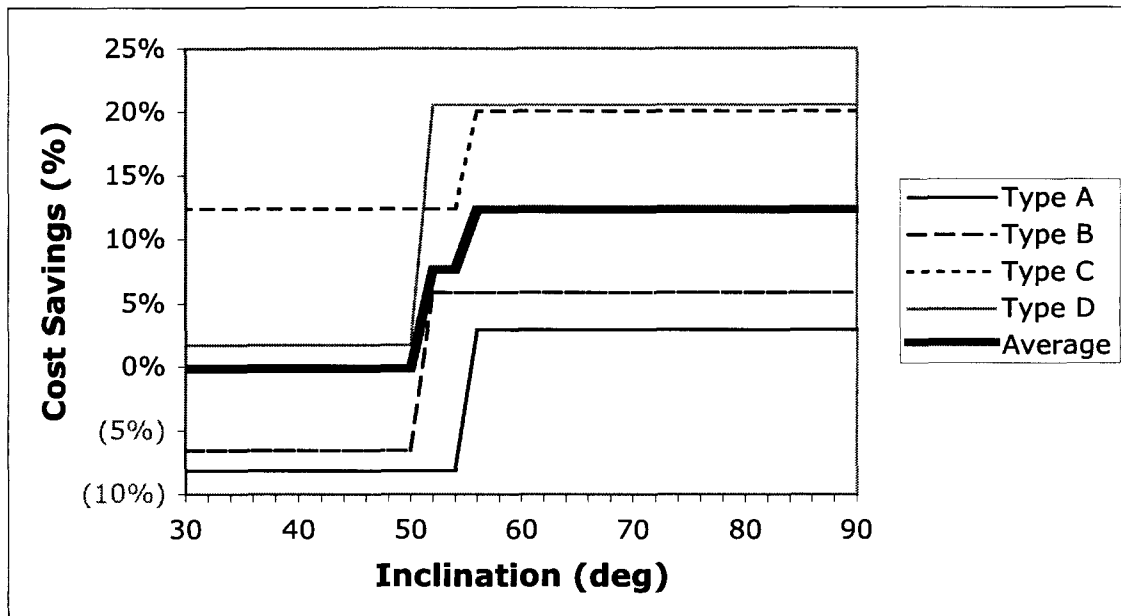


Figure 11: Cost Savings With Respect to Orbit Inclination

CONCLUSIONS

This paper outlined an alternative launch method for microsatellite constellations. The proposed approach offers potential cost savings by utilizing larger, more cost-efficient launch vehicles and taking advantage of the Earth-Moon L1 point to distribute the satellites throughout various orbital planes. The above analysis proves the feasibility of the concept using a basic trajectory design and systems analysis.

While we have demonstrated the feasibility and cost savings of the proposed injection concept, more detailed analysis is necessary. One major challenge is the discovery of separate Earth return trajectories for each final Earth orbital plane. The linear approximation of the equations of motion only holds for short distances from the L1 point; thus, analysis requires a more detailed model of the motion between L1 and Earth. The other key challenge lies in the area of aerobraking into Earth orbit; a more detailed analysis of systems and trajectory design issues is required. Finally, the systems and cost analysis requires major refinements; this analysis proves the feasibility of the concept but is not rigorous enough to project actual cost savings for the proposed launch method. For example, the operations costs associated with the proposed L1 trajectory have not been accounted for. In addition, further consideration of issues such as radiation exposure is necessary.

Nevertheless, the results presented above are sufficient to show that the proposed launch method offers the potential for significant cost savings for certain types of microsatellite constellations. For the baseline case considered above, we find a 38% cost savings over the currently used direct launch method (one launch vehicle per orbital plane). Expanding the analysis over various types (sizes, inclinations, and altitudes) of constellations shows that significant savings can be realized for a large range of constellation designs.

REFERENCES

1. Lemmerman, L. et al. "Advanced Platform Technologies for Earth Science." Presented at the International Aeronautics Association conference, February, 2003.
2. London, Howard S., "Change of Satellite Orbit Plane by Aerodynamic Maneuvering," *Journal of the Aerospace Sciences*, Vol. 29, No. 3, 1962, pp. 323-332.
3. *ELV Mission Analysis Information Launch Vehicle Information*.
<<http://elvperf.ksc.nasa.gov/>>.
4. Richardson, D.L., "A Note on a Lagrangian Formulation for Motion About the Collinear Points" and "Analytic Construction of Periodic Orbits about the Collinear Points," *Celestial Mechanics* 22, 1980, pp. 231-236.
5. Farquhar, R.W. and Kamel, A., "Quasi-Periodic Orbits About the Translunar Libration Point," *Celestial Mechanics* 7, 1973, pp. 458-473.
6. McCuskey, S. W., *Introduction to Celestial Mechanics*. Addison-Wesley, 1963.
7. Gomez, G., Jorba, A., Masdemont, J., and Simo, C., "Study of the transfer from the Earth to a Halo Orbit Around the Equilibrium Point L1," *Celestial Mechanics and Dynamical Astronomy* 56, 1993, pp. 541-562.

8. *Delta IV: Payload Planners Guide*. The Boeing Company: Huntington Beach, CA, October, 2000.
9. Johnson, W. Correspondence with author. NASA Jet Propulsion Laboratory. January, 2004.
10. Wertz, J. and Larson, W., *Space Mission Analysis and Design, 3rd Edition*, Microcosm, 1999.
11. *Rapid Spacecraft Development Office*. <<http://rsdo.gsfc.nasa.gov>>.